Effect of Halide Anions on the Structure and Dynamics of Water Next to an Alumina (0001) Surface

Aashish Tuladhar, Stefan M. Piontek, Laszlo Frazer, and Eric Borguet,*

Department of Chemistry, Temple University, 1901 N. 13th St., Philadelphia, PA 19122, USA

Supporting Information

1. Experimental Section

a. Sample Preparation: α-Al_2O_3 triangular roof prisms (15 x 13 x 13 x 15 mm) with the 15 x 15 mm square face (opposite of the roof) cut at (0001) orientation were purchased from Team Photon Inc. (San Diego, CA). Before the experiment, the α-Al_2O_3 triangular prisms were first cleaned with freshly prepared "piranha" solution (1 vol conc H_2O_2: 3 vol conc H_2SO_4) for ~30 minutes in a Teflon holder. *(**CAUTION**: "piranha" is a very reactive mixture and must be handled with great care by using protective equipment including appropriate gloves, googles, and lab coat.* The prisms were then rinsed with copious amounts of deionized water (>18.2 MΩ·cm resistivity, Thermoscientific Barnstead Easypure II purification system with a UV lamp) and dried by filtered compressed N_2 gas. The prisms were then cleaned with low-pressure RF plasma (Harrick) operated in high RF level setting for ~15 minutes, after which they were kept covered and allowed to equilibrate in ambient at room temperature before experiments. One of the prisms was coated with ~100 nm Au film and used for normalization of the raw data.

The triangular prism was mounted in a flow through sample holder. High grade (>99.99%) salts (NaF, NaCl, NaI, and NaBr) were purchased from Sigma Aldrich and were used as received to prepare 0.1 M solutions. The pH of these 0.1 M salt solutions were adjusted to pH 4 or pH 10 by adding small amounts of pH 2 and pH 12 solutions, respectively and the pHs of the solutions were verified with a pH-meter (Oakton). The pH 2 and pH 12 solutions were prepared from adding deionized water to concentrated HCl (Sigma Aldrich, 37 wt. % in H_2O, 99.999% trace metal basis) and concentrated NaOH (Fluka Analytical, 4M NaOH in H_2O).

b. Optical Setup: The one box Ti:Sapphire oscillator + regenerative amplifier (Coherent, LIBRA –F-1K-110-HE+) produces 5.0 mJ at 800 nm with a pulse duration of 120 fs at a repetition rate of 1 kHz. 90% of 5 mJ (4.5 mJ) is used to pump a commercial OPA (Coherent, TOPAS-Prime HE) to produce 1.3 W of signal and idler output. Tunable mid-infrared pulses are generated by collinear difference frequency generation (DFG) mixing of signal and idler pulses in an $AgGaS_2$ (AGS) crystal with typical pulse energy of 20 μJ @ 3 μm (~230 cm^{-1} FWHM). The mid-IR pulses are divided, using a silicon wedge, to produce pump and probe IR pulses with the power ratio of 3:1. The remaining 5% of the regenerative amplifier output, spectrally narrowed to a FWHM of ~ 2.5 nm using a narrow bandpass filter, is used for vSFG measurements. The IR pump (8 μJ/pulse), IR probe (3 μJ/pulse), and visible (5 μJ/pulse) beams incident at the surface with angles of 58°, 46°, and 51°, were focused to beam waists of ~75, ~75, and 200 μm diameter, respectively. The visible incident angle was chosen to be greater than the critical angle (which was calculated to be ~50° for the 800 nm visible beam at Al_2O_3/H_2O interface using Snell's Law) to ensure enhancement of the vSFG signal via total internal reflection. All incident beams were p-polarized. The p-polarized SFG signal was separated from the reflected visible light by a 750 nm short pass filter (Melles Griot) and was detected by a CCD detector (Princeton Instruments) coupled with a spectrograph (300i, Acton Research Corp.).

In order to cover the entire O-H stretching region (Figure S1) for the steady-state vibrational SFG (vSFG) measurements, the phase matching angle of the AGS crystal and the non-collinearity of the signal and idler beam were adjusted to generate ultra-broad mid-IR output (covering 2800-3700 cm^{-1} region). Only the pump IR and the visible beams were used for acquiring the steady-state vSFG spectra. The mid-IR beam was spatially and temporally

overlapped with a spectrally narrowed (~2.5 nm) 800 nm visible pulses (using a narrow bandpass filter, CVI Laser Optics) at the interface to produce sum frequency photons. The raw vSFG spectrum from the Al_2O_3/H_2O interface was normalized with respect to the IR pulse profile by dividing the raw sample spectrum by a reference spectrum acquired from the Al_2O_3-Au interface under otherwise identical conditions. The normalized spectrum was further corrected for the wavelength dependence of the Fresnel factor.[1-2]

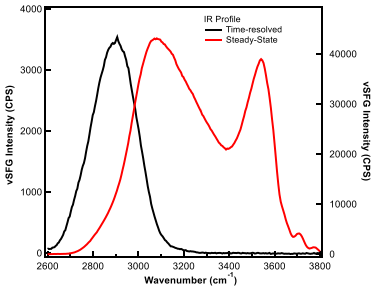

Figure S1-1. IR profile acquired from the Al_2O_3(0001)/Au interface used for the steady-state (red solid line) and time-resolved (black solid line) vSFG measurements.

For the time-resolved vSFG measurements, narrower IR pulses (FWHM ~230 cm^{-1}) centered at 2900 cm^{-1} were used to investigate the strongly hydrogen bonded O-H stretching region (Figure S1-1). Initially, the intense P-polarized IR pump pulse transfers population from the vibrational ground state (ν=0) to the first excited state (ν =1). The vSFG signal generated

from the weaker probe IR and visible pulse monitors the ground-state population as a function of time.

The instrument response function (IRF) was determined from the cross-correlation between IR pump and IR probe, measured using three beam sum frequency generation. The time delay between the IR probe and the visible was fixed, and the IR pump beam was scanned with respect to the IR probe and 800 nm visible for acquiring the IRF and time-resolved vSFG measurements.

The data was recorded in 33 fs time steps using custom written programs with LABVIEW software. In order to account for the laser drift during typical scan time (15 minutes – 1 hour), an external shutter was placed in the pump IR path so that at each acquisition time step, pumped (shutter open) and un-pumped (shutter closed) dynamics data were recorded. The pumped data was divided by un-pumped data to acquire normalized dynamics data.

In the time-resolved vSFG measurements the entire CCD chip is recorded, i.e., a matrix of 1300 x 100 (horizontal and vertical pixels of the CCD) is generated for every time delay from -1 ps to 3 ps (with 33 fs time steps). This time-resolved vSFG data is investigated in two ways:
1) Integrated IR pump-vSFG probe is collected by summing up all the pixels of the CCD for a given time delay, which reduces the 1300x100 matrix into a single value. As a result, a scalar value is generated for a given time delay for both pump on and pump off measurements. Then the pump-on scalar value is divided by pump-off scalar value to generate a normalized vSFG intensity. This is repeated for all the time delays (-1 ps to 3 ps) to generate integrated IR pump-vSFG probe data.
2) Spectrally resolved IR pump-vSFG is collected by only summing up only the vertical pixels of the CCD, which reduces the 1300 x 100 matrix to a 1300 x 1 matrix, i.e., the vSFG spectrum. So

for every time delay, pump-on and pump-off vSFG spectra are generated. The pump-on vSFG spectrum is divided by a pump-off vSFG spectrum to generate a normalized vSFG spectrum for a given time delay. This is repeated for all the time delays (-1 ps to 3 ps) to generate spectrally resolved IR pump-vSFG probe data.

2. vSFG reproducibility experiments

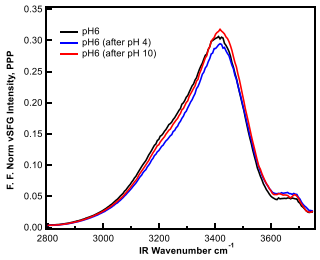

Figure S2-1. vSFG spectra of the α-Al_2O_3(0001)/H_2O (pH 6) at the start of the experiment (black solid line), after pH 4 experiments (blue solid line), and after pH 10 experiments (red solid lines).

Figure S2-2. Two trials of vSFG spectra of the α-Al_2O_3(0001)/H_2O (pH 4) with two different experimental sequences as shown by the respective legends. (Left) Biggest to smallest anion. (Right) Smallest to biggest anion.

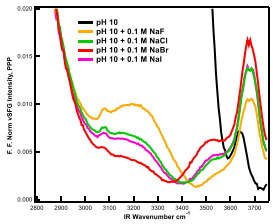

Figure S2-3. Three trials of vSFG spectra of the α-Al_2O_3(0001)/H_2O (pH 10) with two different experimental sequence as shown by the respective legends. (Left) Biggest to smallest anion. (Right) Smallest to biggest anion. (Bottom) Smallest to biggest anion.

3. Fitting of time-resolved vSFG data

a. Four level model used to fit time resolved vSFG measurements

The kinetics of recovery of the bleach for positively charged alumina/water interfaces is clearly double-exponential in nature (Figure 3 and S5-1) as seen previously by Bakker et al. in their bulk water dynamics data,[3] and other IR pump – integrated vSFG probe experiments on the O-H stretch of water.[4-7] Hence, a four-level system[3-7] (Figure S3-1) is used to fit the IR pump-integrated vSFG probe data.

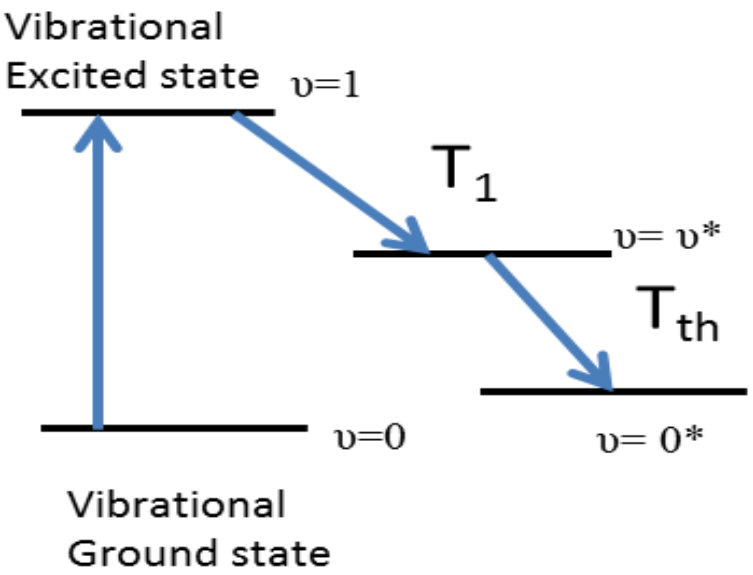

Figure S3-1. Four level model used to describe the vibrational relaxation of water in the bulk and at interfaces

The four coupled differential equations that describe the transfers of population in the four level model are:

$$\frac{dN_0}{dt} = -\sigma I_{pu}(t)(N_0 - N_1) \qquad (S1)$$

$$\frac{dN_1}{dt} = \sigma I_{pu}(t)(N_0 - N_1) - \frac{N_1}{T_1} \qquad (S2)$$

$$\frac{dN_2}{dt} = \frac{N_1}{T_1} - \frac{N_2}{T_{th}} \qquad (S3)$$

$$\frac{dN_3}{dt} = \frac{N_2}{T_{th}} \qquad (S4)$$

where N_0, N_1, N_2, and N_3 are the populations of the ν=0, ν=1, ν*, and ν*=0 states, respectively, σ is the IR cross section of the ground state (ν=0), $I_{pu}(t)$ is the Gaussian temporal profile of the pump pulse with τ = pulse width at half maximum, and T_1 and T_{th} are the characteristic time constants of vibrational relaxation and thermalization processes, respectively.[6]

Solving equations S1-S4 gives expressions for the populations in the four states (N_0, N_1, N_2, and N_3) as a function of time. This is then substituted into the following expression for the vSFG signal, which is convolved with a Gaussian instrument response function trace IRF(t):

$$I_{SFG} = \mathrm{IRF(t)} * [N_0(t) - N_1(t) + C_2N_2(t) + C_3N_3(t)]^2 + I_F \qquad (S5)$$

where C_2 and C_3 are factors related to the nonlinear optical susceptibilities of the intermediate and final levels, and I_F is the vSFG signal level at t=3 ps.[6]

In total, there are nine fit parameters (Table S2-1) for the four level model, out of which N_0 and T_{th} are held fixed at 1.0 and 0.55 ps, respectively. The value of N_0 = 1 is obtained from the initial normalized vSFG signal level (before the arrival of the pump IR). Since our time-resolved experiments are not very sensitive to the thermalization time constant, the value of T_{th} = 0.55 ps is obtained from our previous studies[1-2] and it seems to fit the thermalization component quite well. All the other parameters are free. Figure 3 (main paper) shows that the 4 level model fits the time-resolved vSFG data for the positively charged alumina/water interface very well and the fit parameters for the pH 4 data are given in Table S2-1.

N_0	t_0	σ	τ	C_2	C_3	I_F	T_1	T_{th}
1.0	-0.002 ps	26.6	0.126 ps	0.81	0.68	-0.89	0.116 ps	0.550 ps

Table S3-1. Fit results for the Al_2O_3/H_2O (pH 4) data using the four level model described above. N_0 and T_{th} are held constant while all the other parameters are free.

b. Limitation of four level model

I. Pumping and probing multiple O-H stretches and fast spectral diffusion

The four level model assumes that there is only one kind of excited O-H stretch being pumped and probed. However, this is clearly not the case as at least two types of O-H stretches (<3000 cm^{-1} and >3000 cm^{-1}) lie within the pump and probe bandwidth of the experiment, which is quite obvious when looking at the spectrally resolved IR pump – vSFG probe measurements (Figure S7-1). The presence of two species would not be problematic for the four level model if the kinetics of vibrational relaxation of both species were spectrally homogeneous. T_1 would then be the vibrational lifetime of both species. However, as can be seen from the IR pump–spectrally resolved vSFG probe measurements (Figure S7-1), this is not the case. In fact, the bleach of the <3000 cm^{-1} region temporally overlaps the induced absorption peak. As a result, the maximum bleach of this species is delayed with respect to the >3000 cm^{-1} region. Consequently, the T_1 obtained from fitting the IR pump-integrated vSFG probe measurement with the four level model only gives an apparent vibrational lifetime, and not truly the vibrational lifetime of a single mode. Additionally, since we are only probing part of the O-H stretch and

not the entire O-H stretch region, fast spectral diffusion to the blue-shifted O-H stretch species (outside the probe window) can lead to an apparent lifetime that is shorter than the real lifetime. Irrespective of both of these limitations of the four level model, the effect of F^- on the vibrational relaxation does not depend on the model used to fit the data and hence, our observations are still valid.

II. Fast T_0 component in negatively charged alumina/water interface

The kinetics of recovery of the bleach for the negatively charged alumina/water interface (pH 10) is limited by the IRF close to time zero and therefore, the relaxation kinetics shows at least three different timescales: T_0, T_1, and T_{th} as discussed in the main paper. As a result, the pH 10 data cannot be fit with the four level model discussed above. When attempting to fit the pH 10 data with the four level model, the extracted T_1 lifetime (100 ± 6 fs) is shortened due to the presence of the T_0 component (Figure S3-2, blue dotted line). Clearly, the blue dotted line is not a good fit. When fit procedure was run by holding T_1 = 35 fs, the four level model fits the fast T_0 component, but results in a poor fit for both T_1 and T_{th} components (Figure S3-2, red dotted line). However, when the fit procedure was run by neglecting the T_0 component (using the data mask function in IGOR to reject the first 100 fs data points after the maximum bleach), the four level model fits the data better and T_1 = 126 ± 8 fs is obtained (Figure S3-2, green solid line). The rest of the pH 10 data (with halide salts) were also fit with four level model by neglecting the data associated with the T_0 component (Figure 5).

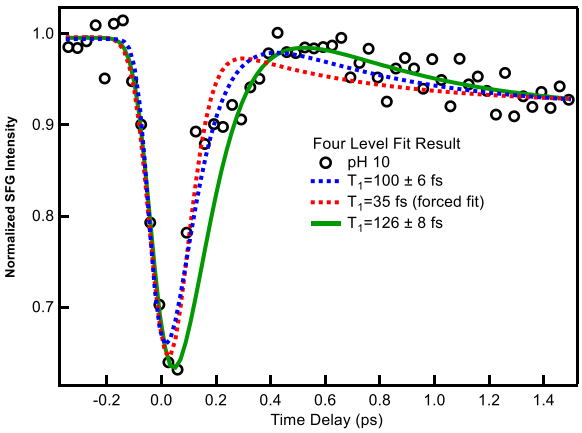

Figure S3-2. IR pump-integrated vSFG probe vibrational dynamics of the interfacial OH species at the α-Al_2O_3(0001)/H_2O interface for bulk pH 10 (black open circles). The lines are best fits with a four-level system, as described in the text above.

4. Definition of time zero in the IR pump-vSFG probe experiments

The time delay t = 0 is defined as the time at which the maximum intensity of the third order cross-correlation ($\chi^{(3)}$) between the IR pump, IR probe, and the visible beam is obtained. The time delay t = 0 can also be defined as the time at which the half of the bleach is reached. However, for our raw data, the maximum of the $\chi^{(3)}$ did not coincide with the half of the bleach

(Figure S4-1). As a result, the time axis for the $\chi^{(3)}$ measurement has been offset by +47 fs and the time axis for the IR pump-vSFG probe measurements has been offset by +160 fs.

Figure S4-1. (Left) Raw $\chi^{(3)}$ and IR pump-vSFG probe data. (Right) Time axis corrected (as described in text above) $\chi^{(3)}$ and IR pump-vSFG probe data.

5. Effect of halide salts on the vibrational dynamics of positively charged Al_2O_3/H_2O interface

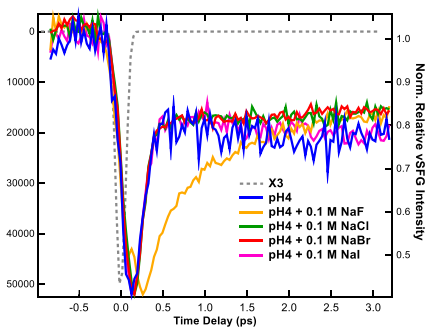

Figure S5-1. Vibrational dynamics of the interfacial OH species at the α-Al_2O_3(0001)/H_2O interface for neat bulk pH 4 (blue) and with 0.1 M NaF (yellow), NaCl (green), NaBr (red), and NaI (pink). The third-order cross-correlation between IR pump, IR probe, and visible is shown by the grey dashed line. P-polarized IR pump and PPP-polarized vSFG probe were used.

6. Effect of halide salts on the vibrational dynamics of negatively charged Al_2O_3/H_2O interface

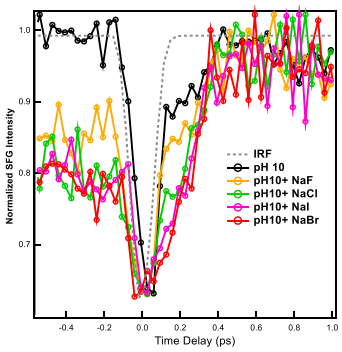

Figure S6-1. Vibrational dynamics of the interfacial OH species at the α-Al_2O_3(0001)/H_2O interface for neat bulk pH 10 (black) and with 0.1 M NaF (yellow), NaCl (green), NaBr (red), and NaI (pink). The data is normalized with respect to the highest vSFG signal. The IRF is shown by the grey dashed line. P-polarized IR pump and PPP-polarized vSFG probe were used. The amplitude of the T_0 component is reduced in the sequence NaBr > NaI > NaCl > NaF, which is identical to the sequence of the attenuated vSFG signal (Figure 2).

7. IR pump-spectrally-resolved vSFG probe measurements of positively and negatively charged Al_2O_3/H_2O interface

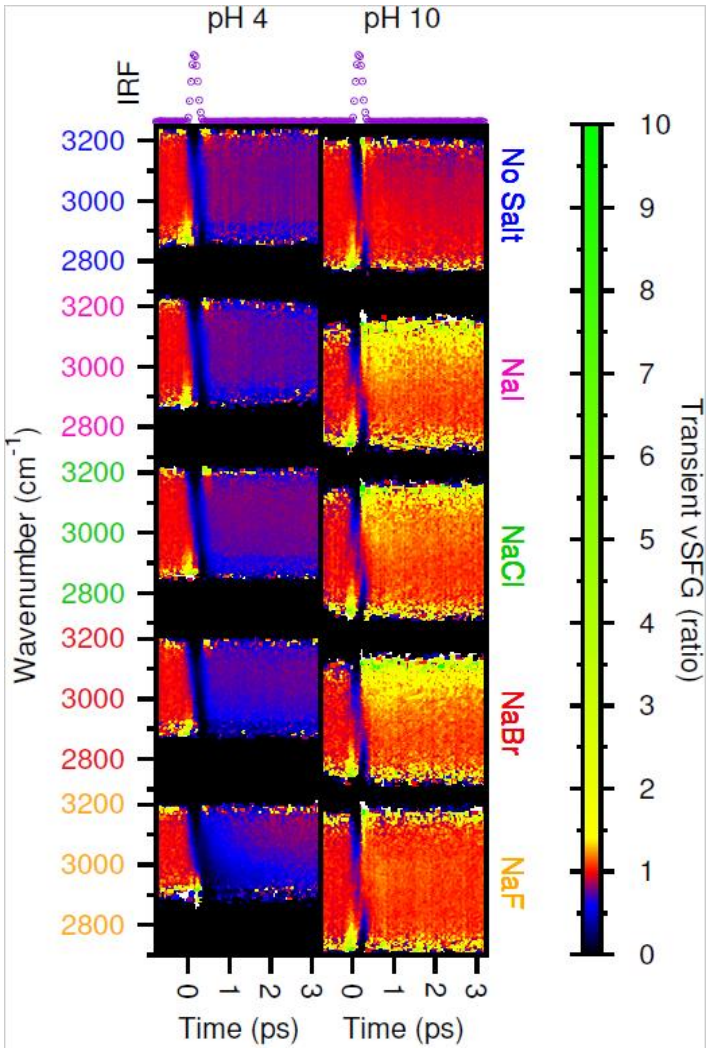

Figure S7-1. IR pump-spectrally resolved vSFG probe vibrational dynamics of the interfacial OH species at the α-Al_2O_3(0001)/H_2O interface for bulk pH 4 (left) and pH 10 (right), displayed from top to bottom without excess salt and with 0.1 M excess NaI, NaCl, NaBr, and NaF. Black indicates zero or no data.

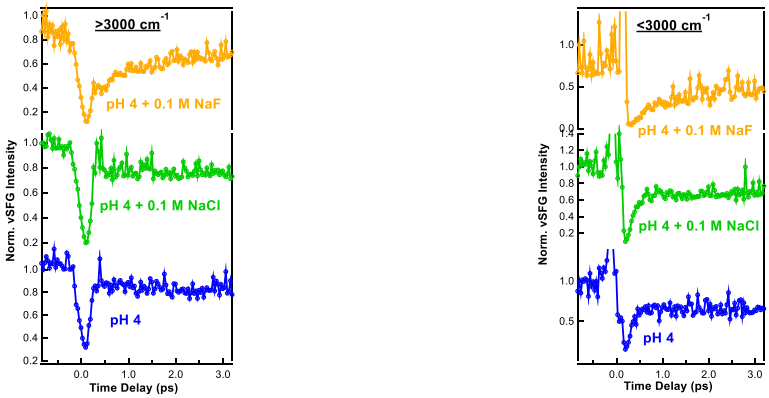

Figure S7-2 Integrating the IR pump-spectrally resolved vSFG probe data for the positively charged α-Al_2O_3(0001)/H_2O interface neat bulk pH 4 (blue) and with 0.1 M NaF (yellow), and NaCl (green). The left graph shows the vibrational dynamics for >3000 cm^{-1} species and the right graph shows the vibrational dynamics for <3000 cm^{-1} species. On the right side, bleach and induced absorption overlap near t=0 as discussed in section 3. b. I. Unlike Figure S5-1, this representation is not weighted by the spectrum of the probe pulse.

8. Effect of halide salts on the vibrational dynamics of positively charged

Al_2O_3/H_2O interface using a blue-shifted IR pump-vSFG probe

In order to test our hypothesis that F^- slows down the vibrational dynamics by mainly affecting the region <2900 cm^{-1}, the IR pump and probe window was slightly blue-shifted (Figure S8-1, SI) to 2900-3300 cm^{-1} (instead of 2800-3100 cm^{-1} region, Figure S1-1) and the integrated time-resolved vSFG measurements were repeated (Figure S8-2).

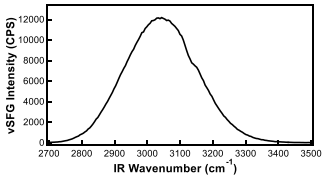

Figure S8-1. IR profile acquired from Al_2O_3(0001)/Au interface used for the blue-shifted IR pump-vSFG probe measurements.

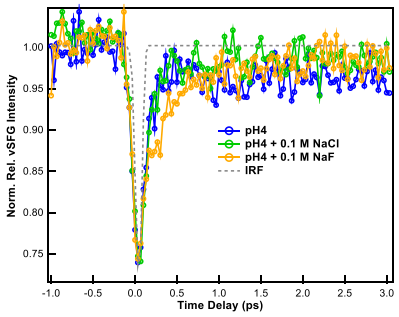

Figure S8-2. Vibrational dynamics of the interfacial OH species at the α-Al_2O_3(0001)/H_2O interface for neat bulk pH 4 (blue) and with 0.1 M NaF (yellow), NaCl (green), NaBr (red), and NaI (pink). P-polarized IR pump and PPP-polarized vSFG probe were used.

1. Tuladhar, A.; Piontek, S. M.; Borguet, E. Insights on Interfacial Structure, Dynamics, and Proton Transfer from Ultrafast Vibrational Sum Frequency Generation Spectroscopy of the Alumina(0001)/Water Interface. *J. Phys. Chem. B* **2017**, *121*, 5168-5177.
2. Tuladhar, A.; Dewan, S.; Kubicki, J. D.; Borguet, E. Spectroscopy and Ultrafast Vibrational Dynamics of Strongly Hydrogen Bonded OH Species at the α-Al_2O_3(11-20)/H_2O Interface. *J. Phys. Chem. B* **2016**, *120*, 16153-16161.
3. Lock, A. J.; Woutersen, S.; Bakker, H. J. Ultrafast Energy Equilibration in Hydrogen-Bonded Liquids. *J. Phys. Chem. A* **2001**, *105*, 1238-1243.
4. Eftekhari-Bafrooei, A.; Borguet, E. Effect of Surface Charge on the Vibrational Dynamics of Interfacial Water. *J. Am. Chem. Soc.* **2009**, *131*, 12034-12035.
5. McGuire, J. A.; Shen, Y. R. Ultrafast Vibrational Dynamics at Water Interfaces. *Science* **2006**, *313*, 1945-1948.
6. Eftekhari-Bafrooei, A.; Borguet, E. Effect of Electric Fields on the Ultrafast Vibrational Relaxation of Water at a Charged Solid–Liquid Interface as Probed by Vibrational Sum Frequency Generation. *J. Phys. Chem. Lett* **2011**, *2*, 1353-1358.
7. Smits, M.; Ghosh, A.; Bredenbeck, J.; Yamamoto, S.; Müller, M.; Bonn, M. Ultrafast Energy Flow in Model Biological Membranes. *New Journal of Physics* **2007**, *9*, 390.